Journal of Water Resource and Protection, 2012, 4, 231-247
http://dx.doi.org/10.4236/jwarp.2012.44026 Published Online April 2012 (http://www.SciRP.org/journal/jwarp)

Conceptual Hydrogeological Model and Groundwater Resource Estimation in a Complex Hydrothermal Area: The Case of the Viterbo Geothermal Area (Central Italy)

Antonella Baiocchi, Francesca Lotti, Vincenzo Piscopo*
Dipartimento di Scienze Ecologiche e Biologiche (DEB), Università degli Studi della Tuscia, Viterbo, Italy
Email: *piscopo@unitus.it

Received February 1, 2012; revised March 2, 2012; accepted April 2, 2012

ABSTRACT

The conceptual hydrogeological model of the Viterbo thermal area in central Italy and the yield of the groundwater system have been examined. This area is of great geothermal interest. Through new investigations, three overlapping aquifers have been found. This study examines in detail the two shallower aquifers, characterized by different hydraulic and chemical characteristics. The first aquifer is related to the regional groundwater flow of the Cimino-Vico volcanic system and is generally characterized by cold, fresh waters used for irrigation and drinking water supply. The second aquifer, *i.e.* the thermal aquifer, supply thermal spas and public pools; it is present where the local hydrostratigraphic, structural and geothermal conditions permit a relatively active flow of higher salinity thermal waters (40˚C - 62˚C). These two aquifers interact vertically and laterally, giving rise to mixed waters circulating in the first aquifer. The first aquifer is recharged by direct infiltration and inflow from regional groundwater, as well as inflow from the second aquifer. The yield of the thermal aquifer is at least 170 L/s, discharging into thermal springs and wells, besides feeding the shallow aquifer vertically and laterally. Even if a future development of the second aquifer is potentially achievable on a global scale, the exploitation of the thermal waters is strictly dependent on the specific local hydrogeological equilibrium between the overlapping aquifers, different from place to place. The case study highlights that, in the volcanic hydrogeological environment, one of the most stringent constraints in determining the correct usage of a resource is the variable level of interaction of groundwater with different qualities.

Keywords: Volcanic Aquifer; Thermal Waters; Overlapping Aquifers Interaction; Viterbo; Italy

1. Introduction

The city of Viterbo is in the Tuscany-Latium geothermal region and is of great geothermal interest [1]. Several thermal springs and wells are present that have water temperatures as high as 62˚C. Some of these springs have been known for their therapeutic properties since Roman times, and wells have been drilled for geothermal exploration since the 1950s.

Currently, these thermal waters are used primarily to supply thermal spas and public pools. In the same area, a shallow aquifer carries cold and fresh water, which is used for irrigation and the local drinking water supply. Increases in spa tourism and the use of geothermal energy are expected in the near future. This multi-purpose water demand also exists for other volcanic aquifers in Italy and around the world e.g., [2-7]. To address the future groundwater management in these complex systems, it is important to examine the local response of the aquifers to withdrawals.

The purpose of this paper is to review the conceptual hydrogeological model of the Viterbo thermal area and to estimate the yield of the groundwater system. This study represents a first step toward determining criteria for the sustainable management of groundwater in this area using a numerical model. Various studies of the Viterbo thermal area have addressed the reconstruction of the stratigraphy and structure, the evaluation of heat flow, the chemical characteristics of gaseous and hydrothermal emissions, and the origin of the thermal waters. However, because of the lack of complete data, few hydrogeological studies have defined the interactions between aquifers and the yield of the system. These aspects are studied herein through new investigations using an integrated approach that combines a hydrogeological and hydrochemical characterization of the complex groundwater system.

2. Geological and Hydrogeological Outlines

The study area lies between the Tyrrhenian coast and

*Corresponding author.

the Apennine Mountains (**Figure 1(a)**). This region contains a series of sedimentary basins related to the processes that occurred during the formation of the Apennine Chain. Periods of local subsidence alternated with periods of differential uplift and intense volcanic activity have affected the region since the Pliocene [8-11]. Volcanic activity gave rise to the Cimino and Vico complexes (**Figure 1(a)**); the former is related to the Tuscan-Roman anatectic magmatic province, and the latter is related to the Roman-Campanian potassic alkaline province [12-15].

The Cimino complex was active between 1.35 and 0.95 Ma. Effusive and explosive activity gave rise to several domes that developed along a NW-SE trending fracture and included pyroclastic deposits. Rhyodacitic ignimbrites and domes as well as latitic and olivinelatitic lavas constitute the volcanic complex [16-18].

The Vico complex consists of a stratovolcano with a central caldera that houses Vico Lake. This volcano was mainly active between 419 ka and 95 ka and developed along a NW-SE elongated graben at the intersection with a NE-SW fracture. Alternating explosive and effusive phases gave rise to several pyroclastic deposits and lava flows, which are phonolitic, tephritic and trachytic in composition [18-21].

The thickened folded and thrusted substratum beneath the Cimino and Vico volcanics is composed of Mesozoic-Cenozoic carbonate sequences (that are several thousands of meters thick) and siliciclastic turbidite deposits (the Upper Cretaceous-Eocene flysch) [9,10,22-25]. NW- and NE-striking extensional faults subdivide the substratum rocks and control the horst and graben pattern. Neogene-Quaternary marine to continental deposits fill the structural low of the Mesozoic-Cenozoic units.

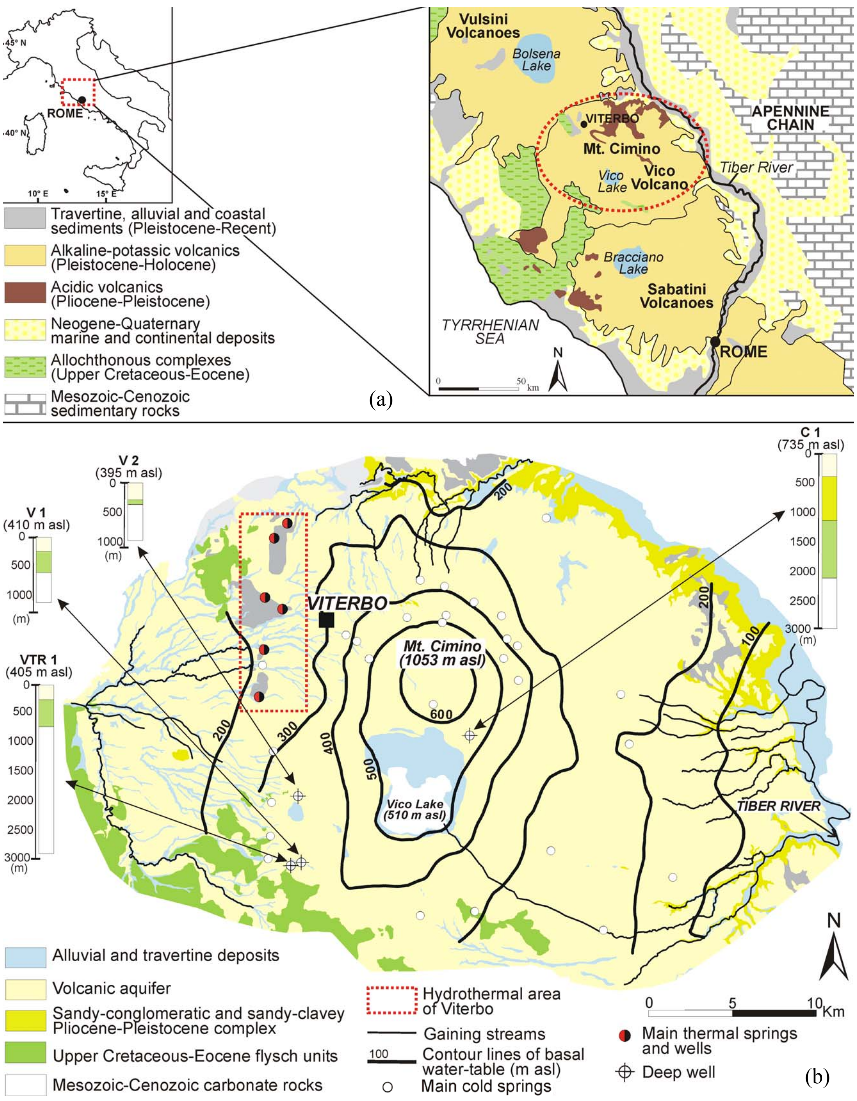

Figure 1. (a) Cimino-Vico volcanoes location in central Italy; (b) Simplified hydrogeological map of the Cimino-Vico system [34] with location of hydrothermal area of Viterbo.

The thinning of the lithosphere and the related igneous processes affecting the pre-Apennine belt explain the formation of the strong regional heat flow anomaly. Values of heat flow between 200 and 300 mW/m^2 over wide areas and up to 400 mW/m^2 in smaller zones have been recognized [1,26-28].

Substantial CO_2 emissions characterize the area and control the genesis of the travertine [29-33] that typically outcrops around the Viterbo thermal area (**Figure 1(b)**).

The Cimino and Vico volcanites constitute an aquifer system limited by the Pliocene-Pleistocene sedimentary complex and Upper Cretaceous-Eocene flysch units (**Figure 1(b)**). A continuous basal aquifer and several limited, discontinuous perched aquifers are present [34-36]. The volcanic aquifer discharges mainly into streams and springs, and it flows towards the alluvial aquifer. The mean yield of the volcanic aquifer has been estimated to be between 5 and 7 m^3/s [34].

In the study area, the Mesozoic-Cenozoic carbonate rocks are considered to be a deep aquifer hosting a thermal reservoir [26,37-38]. The shallow and deep aquifers are separated by thick low-permeability Pliocene-Pleistocene and Upper Cretaceous-Eocene sedimentary rocks. West of Viterbo, the uplift of the basement of the volcanites and the high heat flow are considered to be the origin of the uprising of thermal waters via faults and fractures (**Figure 1(b)**). Sulfate-alkaline-earth-type thermal waters with temperatures between 50˚C and 62˚C are more mineralized and have higher gas contents (CO_2 and H_2S). By contrast, the waters of the volcanic aquifer comprise fresh and cold bicarbonate-alkaline-earth waters [37,39, 40].

3. Methods and Data

Based on the present knowledge of the Viterbo thermal area, new investigations were planned, including: 1) hydrostratigraphic data acquisition; 2) flow and water level measurements; 3) pumping tests; 4) chemical and isotopic analyses; and 5) meteorological, soil and land use data processing.

The hydrostratigraphy of the area was reconstructed based on available studies and the interpretation of 62 lithologic logs. These logs concern wells and boreholes with depths ranging from tens to hundreds of meters and report information on the stratigraphy, aquifer formations, water level and, in some cases, water temperature.

Flow measurements were conducted in August-October 2008, May-June 2009 and September 2010 for 15 thermal springs, 9 cold springs, 7 flowing thermal wells and 28 stream sections. Measurements with an accuracy of 5% to 10% were obtained using tanks or current meters.

The water level, temperature and electrical conductivity in the wells were measured in August-October 2008 and May-June 2009 with a multiparametric probe. For the flowing wells, the water level was determined according to the fluid pressure measured with a manometer. In total, 130 wells with depths of 5 to 150 m were measured in or near the hydrothermal area.

Pumping test results at five wells that penetrate the shallow volcanic aquifer were acquired from the literature. Two new pumping tests were performed to monitor the temperature and/or electrical conductivity of the pumped water. Six other step-drawdown tests were also conducted for the same aquifer.

Three new pumping tests were also performed on the thermal wells. Two tests were conducted at a constant rate with observation piezometers or springs to monitor the chemical and physical characteristics of the water at each point. A third test was conducted by opening and closing a flowing well and observing the response of a second well.

Water from a total of 52 sources was sampled during a survey conducted in June 2009 and during the pumping tests.

The temperature, pH and electrical conductivity were measured in the field using portable meters. The alkalinity was determined on-site by means of titration.

Major anions (Cl^-, SO_4^{2-}), nitrate (NO_3^-) and fluoride (F^-) were determined by ion chromatography using a Dionex-DX-120 system. Major cations (Na^+, K^+, Ca^{2+}, Mg^{2+}), Sr, Li and Fe liquid were determined by atomic absorption spectrophotometry with a Perkin-Elmer 2100 system. SiO_2 was determined with a Secomann S. 500 photocolorimeter. The analytical accuracy of these methods ranges from 2% to 5%, and the charge balance errors were generally less than 5%.

The CO_2 and H_2S dissolved gases were determined for 12 thermal springs and wells. The CO_2 was determined according to the method reported in Capasso and Inguaggiato (1998) [41] using a gas chromatograph for analyticcal measurements. H_2S was stabilized with zinc acetate and determined in the laboratory by means of titration.

Selected environmental isotopes were analyzed in 24 of these samples. Stable isotopes of water, ^2H and ^{18}O, and ^{18}O and ^{34}S of dissolved sulfate were determined by mass spectrometry. The standards used were V-SMOV for oxygen and hydrogen and V-CDT for sulfur. ^{18}O of water was determined on CO_2 isotopically equilibratum with H_2O [42], and ^2H was determined from H_2 produced by the Zn-reduction method. For ^{34}S analyses, SO_4 was prepared using the methods of Yanagisawa and Sakai (1983) [43], and ^{18}O of sulfate was measured from CO_2 prepared by graphite reduction of $BaSO_4$. All values are reported by delta notation (δ‰). The analytical error is estimated to be less than ±1%.

For 15 samples, the tritium concentration was also determined. The samples were distilled, enriched and vacuum-distilled before a liquid scintillation cocktail was added. Analyses were performed using a Perkin-Elmer liquid scintillation counter for twelve 120-min cycles [44]. The results were reported in tritium units (TU).

The air temperature and rainfall data for the area were obtained from the SIMN (Italian hydrographic survey) for the period 1951-1999 [45] and from Regione Lazio for 2000-2010 [46]. The data from the Viterbo meteorological station (327 m asl) were statistically processed to analyze the homogeneity of the data series by applying the cumulative residuals method, and gaps were filled in to complete the series [47,48].

The soil characterization was obtained from the literature [49-51], and the land use information was derived from the Regione Lazio GIS [52].

4. Results

4.1. Hydrostratigraphic Setting

The surface geology grouped by hydrogeological terms is given in **Figure 2(a)**. The sedimentary substratum of the Pleistocene volcanites, together with the likely faults and fractures, are shown in **Figure 2(b)**, as found in the literature [9,53-56] and in the examined lithologic logs. Representative hydrogeological cross-sections are shown in **Figure 3**.

The analysis of cross-section and well data highlights a shallow unconfined or leaky aquifer (referred to as the Shallow Aquifer or SA) up to tens of meters thick. The aquifer is contained within the Pleistocene volcanites, which mainly consist of ignimbrites, tuffs and lava flows.

Below the first aquifer, a second confined aquifer (**Figure 3**) is characterized by thermal waters (referred to as the Thermal Aquifer or TA). This aquifer is intercepted by deeper wells within the volcanites, at the contacts between the volcanites and the flysch units or within the upper portion of the same flysch units, which mainly consist of claystones, marls, marly limestones, sandstones and siliceous limestones.

A low-permeability layer with a thickness of a few meters to tens of meters divides the SA from the TA and is composed of hydrothermally altered pyroclastic deposits or clayey layers of the flysch units.

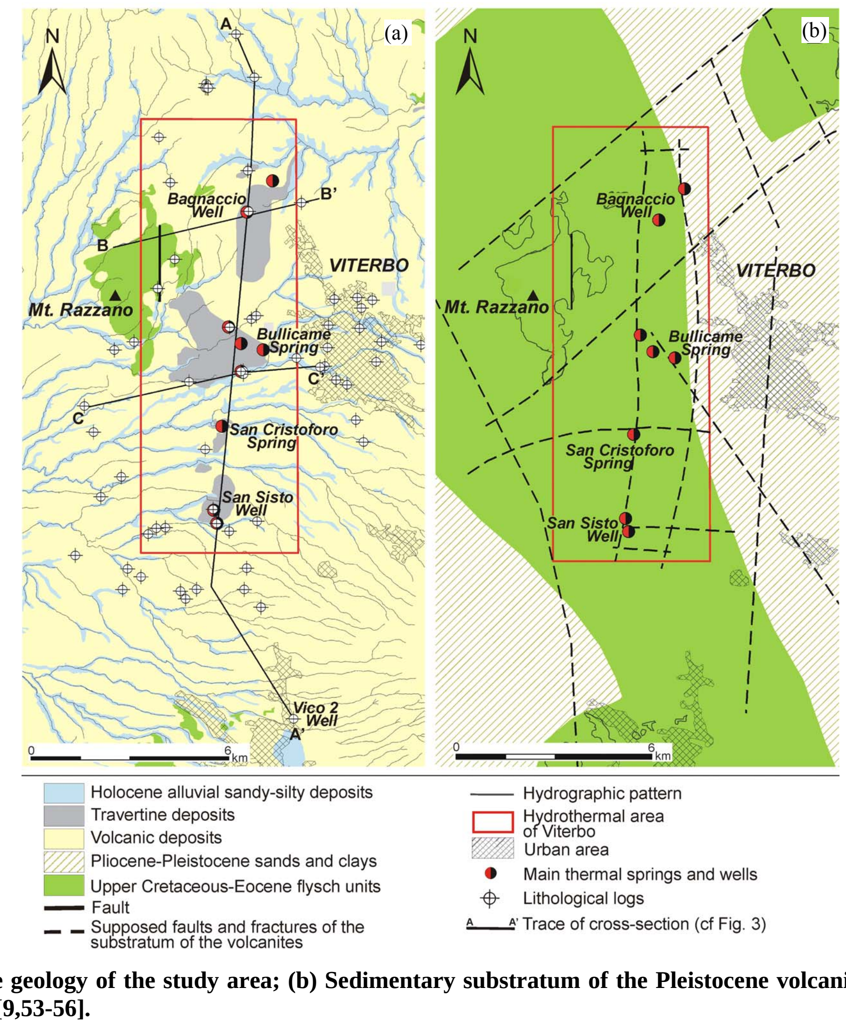

Figure 2. (a) Surface geology of the study area; (b) Sedimentary substratum of the Pleistocene volcanites with the supposed faults and fractures [9,53-56].

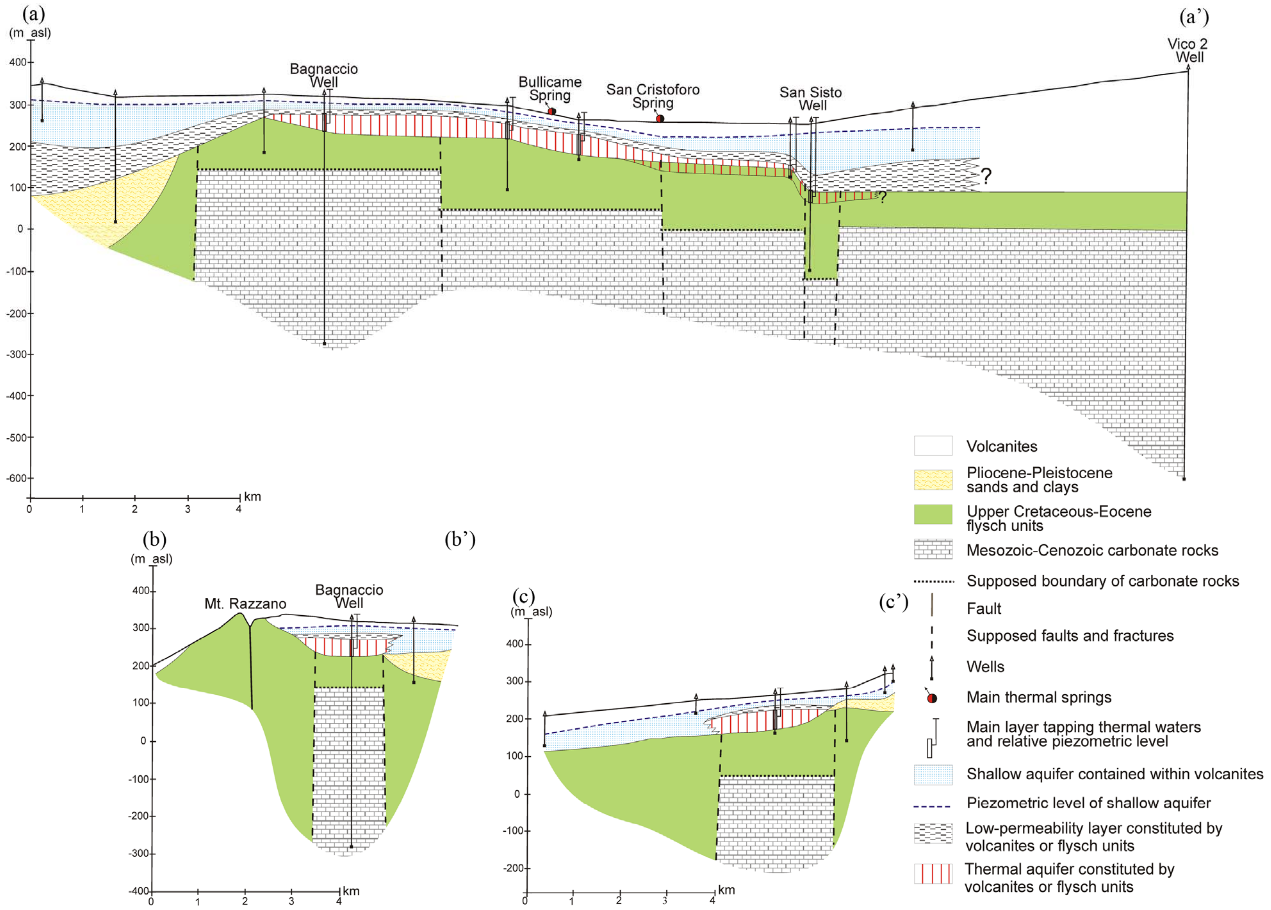

Figure 3. Hydrogeological cross-sections N-S (a-a') and W-E oriented (b-b', c-c'), showing the hydrostratigraphy of the study area.

A third aquifer can be recognized within the deep carbonate rocks, which include limestones, marly limestones, marls, dolomitic limestones, dolostone, and anhydrites. Thermal flow was found in boreholes intercepting this aquifer. In the Bagnaccio Well (**Figure 3**), the thermal flow was lower than that intercepted in the volcanites and in the flysch units [53,54,57]. In the Vico 2 Well (**Figure 3**), the thermal flow had the same temperature as that found in the volcanites (62˚C) [57]. In Vico 1 Well (V1 in **Figure 1(b)**), water with a temperature between 50 and 65˚C was found in the carbonate rocks [57]. In Vetralla 1 Well (VTR1 in **Figure 1(b)**), a production test at a depth of 1130 - 1145 m in the carbonate rocks gave a maximum discharge of approximately 15 L/s and a temperature of 61˚C [38].

In the Vulsini volcanic area, which is tens of kilometers from the study area, the same Mesozoic-Cenozoic carbonate rocks were recognized as the deep reservoir that feeds two deep geothermal wells characterized by Na(K)-Cl water with a high temperature (120˚C - 230˚C) and salinity (6 - 12 g/L) [58-63].

The volcanic basement is uplifted, and the flysch units have relatively reduced thicknesses in the hydrothermal area of Viterbo. The SA overlies thick flysch units to the west and low-permeability Pliocene-Pleistocene units to the east, which are mainly constituted by sands and clays. Deep wells east or west of the uplifted block do not tap thermal flow (**Figure 3**).

4.2. Flow and Water Level Measurements

The location of the flow and water level measurements conducted between 2008 and 2010 is shown in **Figure 4**. **Table 1** summarizes the results of the flow measurements.

Thermal water discharges are grouped into zones (**Figure 4(b)**), and their average values during 2008-2010 are compared with those from 1983-1984 (**Table 1**).

The cold water discharge is computed from the springs and gaining streams in the area (**Table 1** and **Figure 4(a)**). One of the springs, Pidocchio Spring, can be related to the basal water table of the SA if the elevation of the spring (238 m asl) is compared with the piezometric level measured in the neighboring shallow wells; the other springs

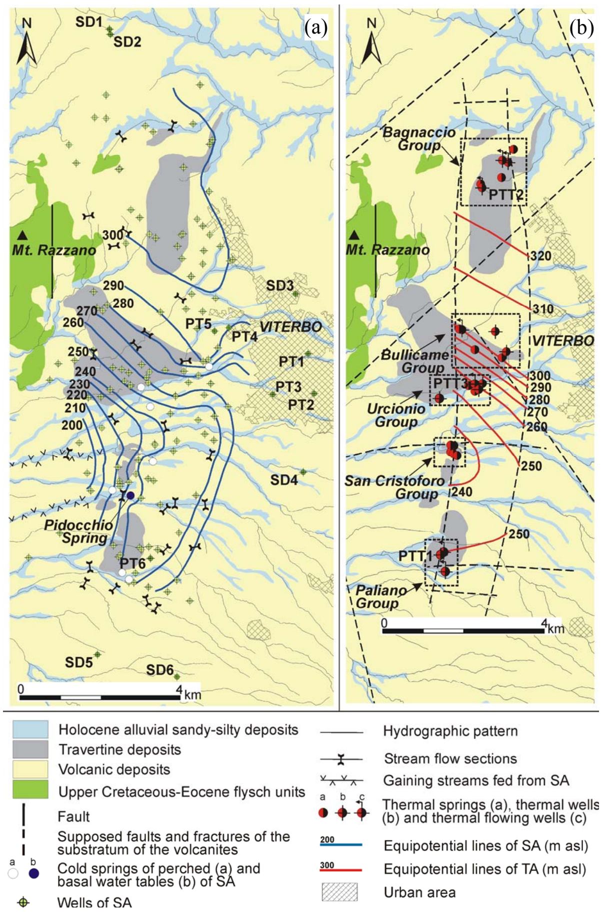

Figure 4. Location of the flow, water level measurements and pumping tests with equipotential maps reconstructed for (a) the shallow aquifer, SA; and (b) Thermal aquifer, TA.

Table 1. Results of flow measurements conducted during 2008-2010 (T: temperature; Q: discharge).

Thermal springs and flowing thermal wells				
Group of springs and wells	Elevation (m·asl)	T (˚C)	Q (L/s) 2008-2010	Q (L/s) 1983-1984[a]
Bagnaccio Group	310 - 320	34 - 62	10.3	17.2
Bullicame Group	284 - 300	40 - 61	29.9	42.3
Urcionio Group	260 - 269	41 - 55	22.8	18.3
S. Cristoforo Group	225 - 242	35 - 54	2.6	1.8
Paliano Group	240 - 255	54 - 59	13.2	9.0
Total discharge (L/s)			78.8	88.6

Springs and increases of streamflow of the shallow aquifer			
Type	Elevation (m·asl)	T (˚C)	Q (L/s)
Spring of basal water-table (Pidocchio Spring)	238	17	12.5
Springs of perched water-tables	240 - 284	16 - 32	4.0
Increase of stream flow	<240		90.7
Total discharge (L/s)			107.2

[a]From Camponeschi and Nolasco (1984) [57].

are related to the perched aquifers of the volcanites. A significant flow arising from the discharge from the basal water table of the SA was measured in the streams of the southern zone during the dry season of 2008 (**Figure 4(a)**).

The first equipotential map of the SA is based on wells containing water below 23˚C. The second map includes wells with temperatures up to 31˚C (**Figure 4(a)**) but is not significantly different from the first map. The equipotential map shows a general conformity of the water-table contours with the topography. The hydraulic gradient varies between 0.006 and 0.06.

A rough potentiometric surface of the TA is given in **Figure 4(b)**. This reconstruction is based on the measurements of the water level or fluid pressure of the deeper wells and the elevation of the springs, which both have water temperatures above 40˚C. The map shows two main directions of flow, one oriented NE-SW and a second oriented SE-NW, that converge toward the western boundary of the hydrothermal area.

By comparing the equipotential maps of the TA and SA, a difference in the hydraulic head between 5 and 20 m can be estimated. The values for the vertical gradient are between 0.2 and 1 with a thickness of the low-permeability layer up to 40 m.

4.3. Pumping Tests

The wells used for the pumping tests on the SA are reported in **Figure 4(a)**. The test results are given in **Table 2**.

Table 2. Results of pumping tests of shallow and thermal wells.

Shallow wells used for pumping tests				
Well	Q (L/s)	b (m)	Transmissivity (m^2/s)	Storativity
PT 1[a]	0.35	26	2.6×10^{-4}	1.2×10^{-3}
PT 2[a]	0.43	17	1.3×10^{-4}	7.8×10^{-3}
PT 3[a]	1.25	34	3.0×10^{-3}	7.9×10^{-3}
PT 4[a]	14.0	14	1.1×10^{-2}	-
PT 5[a]	9.7	20	2.3×10^{-2}	1.8×10^{-3}
PT 5	20	20	4.5×10^{-2}	6.9×10^{-2}
PT 6	7.7	46	5.4×10^{-3}	5.9×10^{-3}
Shallow wells used for step-drawdown tests				
Well	Q (L/s)	b (m)	Specific capacity (m^2/s)	Transmissivity (m^2/s)
SD 1	26	54	2.6×10^{-2}	2.2×10^{-2}
SD 2	25	60	7.8×10^{-3}	5.2×10^{-3}
SD 3	4	40	4.0×10^{-3}	2.4×10^{-3}
SD 4	2	20	1.5×10^{-4}	4.8×10^{-5}
SD 5	2	29	3.3×10^{-4}	1.2×10^{-4}
SD 6	5	21	5.0×10^{-4}	2.0×10^{-4}
Thermal wells used for production tests				
Well	Q (L/s)	b (m)	Transmissivity (m^2/s)	Storativity
PTT 1	38.6	35	8.0×10^{-4} 1.0×10^{-3}	2.0×10^{-4} 3.6×10^{-4}
PTT 2	46.4	55	1.4×10^{-2} 2.8×10^{-2}	-
PTT 3	21.5	30	3.9×10^{-3}	-

[a]from Piscopo *et al.* 2006 [37]; Q: discharge; b: saturated thickness.

Five pumping tests (PT1-PT6 in **Table 2**) were acquired from Piscopo *et al*. (2006) [37]. The new test conducted on PT5 reveals an increase in temperature from 16.0˚C to 16.8˚C after 25 hours of pumping and hydraulic parameters comparable to those previously determined. The test conducted on PT6 did not show an increase in temperature or electrical conductivity during pumping.

Six other step-drawdown tests were conducted on the SA (SD1-SD6 in **Table 2**), and the specific capacity was determined. Using the relationship between transmissivity and specific capacity found for the Cimino-Vico system [34], transmissivity was determined (**Table 2**).

The tests conducted on wells that intercept thermal waters (PTT1, PTT2 and PTT3) are shown in **Figure 4(b)**, and the results are given in **Table 2**.

The PTT1 test was conducted at a constant flow for 68 hours on a 125-m-deep well that penetrates fractured flysch formations. The monitored wells and springs are shown in **Figure 5(a)**. The piezometer at the SA and the thermal springs of the San Cristoforo Group did not show significant variations. The San Sisto Well, which is a thermal flowing well, dried up during the pumping and flowed again after the shutdown of the well (**Figure 5(b)**). The electrical conductivity and temperature of the thermal water were constant in the pumped and observation wells (**Figure 5(c)**). Other chemical and isotopic parameters did not exhibit significant variations during the pumping period.

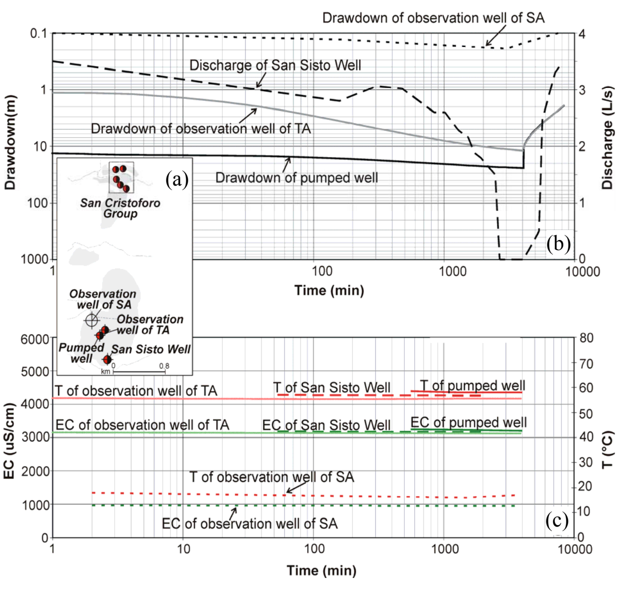

Figure 5. Results of the pumping test conducted on PTT1 well: (a) Location of monitored wells and springs; (b) Trend of drawdown in the tested well and in two observation piezometers, and of discharge of the San Sisto Well; (c) Trend of temperature (T) and electrical conductivity of waters (EC) of the monitored wells.

The best match of drawdown data from the observation well of the TA was obtained at a transmissivity of 8 × 10^{-4} to 1 × 10^{-3} m^2/s and a storativity of 2 to 4 × 10^{-4} by applying the double porosity model.

The PTT2 test was conducted on the Bagnaccio Well, which was drilled during geothermal exploration during the 1950s [53,54]. The Bagnaccio Well was originally 600 m deep, and it was recently (2008) renovated to a depth of 100 m to better capture the thermal water from the volcanites. The flowing well was tested for 48 hours at a constant rate by measuring the fluid pressure (results in **Figure 6**). When the flowing well was closed, the pressure immediately returned to its initial value. During the test period, the physical-chemical characteristics of the water and the other monitored chemical and isotopic parameters did not change. Among the wells and springs monitored during the pumping, only the Bagnaccio Spring (78 m from the well) showed a significant variation (**Figure 6**).

An approximate transmissivity of 2.8 × 10^{-2} m^2/s was estimated by applying the Cooper-Jacob method to the drawdown data measured in the production well. The distance-drawdown method, which was applied considering the Bagnaccio Spring as a piezometer, permitted to determine transmissivity values between 1.4 × 10^{-2} and 2.3 × 10^{-2} m^2/s (**Table 2**).

A third test on the thermal aquifer was conducted in the central zone (PTT3 test) by closing a well that normally flows six days a week at a constant rate of 21.5 L/s. Recovery was observed at a second well 129 m away. The two wells are 42 and 93 m deep and capture thermal water from the volcanites. The transmissivity was estimated to be 3.9 × 10^{-3} m^2/s when considering the residual

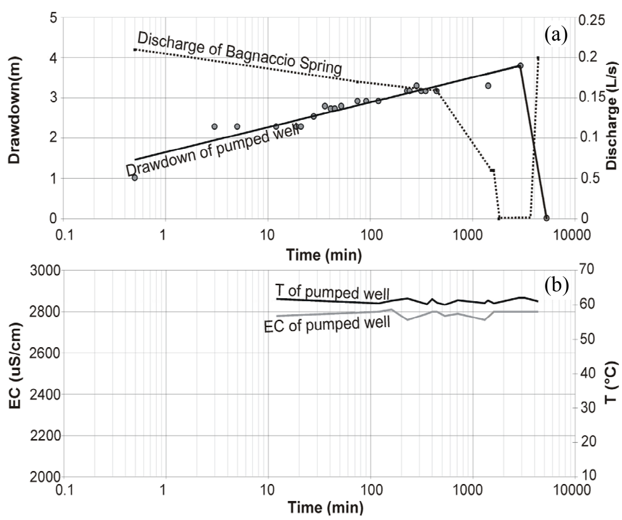

Figure 6. Results of the pumping test conducted on PTT2 well: (a) Trend of drawdown in the tested well and of discharge of the Bagnaccio Spring; (b) Trend of temperature (T) and electrical conductivity of waters (EC) of the tested well.

drawdown in the second well, the times since the initiation and termination of pumping, and the discharge of the flowing well.

4.4. General Chemistry

The main chemical constituents of all of the samples are provided in **Table 3**. The samples were categorized as one of the following: thermal water (spring, *ts*, and well, *tw*) from TA; spring (*s*) and well (*w*) of the SA; and stream waters (*st*). The location of the sampled water is shown in **Figure 7**.

According to the physical-chemical characteristics and the relative abundance of major cations and anions, the thermal waters (also including the waters of Bagnaccio Pond, 7 in **Table 3** and **Figure 7**, which are influenced by the flow of the SA) exhibit a homogenous hydrochemical facies. They are calcium-sulfate waters (**Figure 8**) that are characterized by a temperature (T) of 40˚C to 62˚C, a pH less than 7, and a specific electrical conductivity (EC) between 2800 and 3600 µS/cm.

Wells and springs fed from the SA show a more heterogeneous hydrochemical facies and range from calcium-alkaline-bicarbonate to calcium-sulfate waters (**Figure 8**), with a T of 16˚C to 31˚C, pH up to 8, and EC of 300 to 2900 µS/cm. The two sampled streams have opposite geochemical profiles: one is recharged by the SA (*i.e.*, 15 in **Table 3** and **Figure 7**), whereas the other also by the TA (*i.e.*, 32 in **Table 3** and **Figure 7**).

Among the minor and trace constituents, Li (generally between 0.01 and 0.1 mg/L) and Fe (generally between 0.01 and 0.2 mg/L) are present at very low concentrations. The NO_3^- concentration is lower in thermal waters (generally less than 5 mg/L) than in the waters of the SA (up to 100 mg/L, relative to the depth of the water level below the ground). The SiO_2 concentration varies between 40 and 55 mg/L for thermal waters and is generally lower for the other waters. The strontium concentration is higher in thermal waters, as is the fluoride concentration (**Table 3**).

The Pearson correlation matrix of the entire dataset shows a strong correlation among EC, T, Mg^{2+}, SO_4^{2-}, Sr, and HCO_3^- ($R > 0.8$). The plot of Sr versus the sulfate concentration in **Figure 9** highlights one of these correlaons.

The concentrations of dissolved CO_2 and H_2S gas in the 12 thermal waters (4, 8, 9, 14, 16, 18, 20, 30, 34, 44, 45, 48 in **Figure 7**) vary between 300 and 600 mg/L and 7 and 30 mg/L, respectively.

The highest values were found in the deeper wells that had proper screening, casing and sealing.

These results agree with the previous hydrochemical characterization [37,40] and further highlight that the geochemical profile of the waters of the SA appears to be influenced by mixing with thermal waters (**Figures 8** and **9**). To analyze this point thoroughly, sulfate content was considered as one of the constituents that discriminates the different waters (see also the stable isotope analysis). The following relationship, which has been used in the literature to determine the components of stream flow [64], was applied:

$$Ci \cdot Qi = Ct \cdot Qt + Cc \cdot Qc \quad (1),$$

where

Ci is the sulfate concentration in water sampled from the SA;

Ct is the average sulfate concentration of the thermal waters (1193 mg/L) and is one of the end members;

Cc is the sulfate concentration in Pidocchio Spring (39 in **Table 3** and **Figure 7**), which represents the other end member (19 mg/L), *i.e.*, cold water from the SA that is not influenced by the thermal flow;

Qi is the total flow rate of the SA;

Qt is the component of the flow rate of thermal waters in the SA; and

Qc is the component of the flow rate of cold waters in the SA.

Considering that $Qi = Qt + Qc$, Equation (1) can be rewritten as

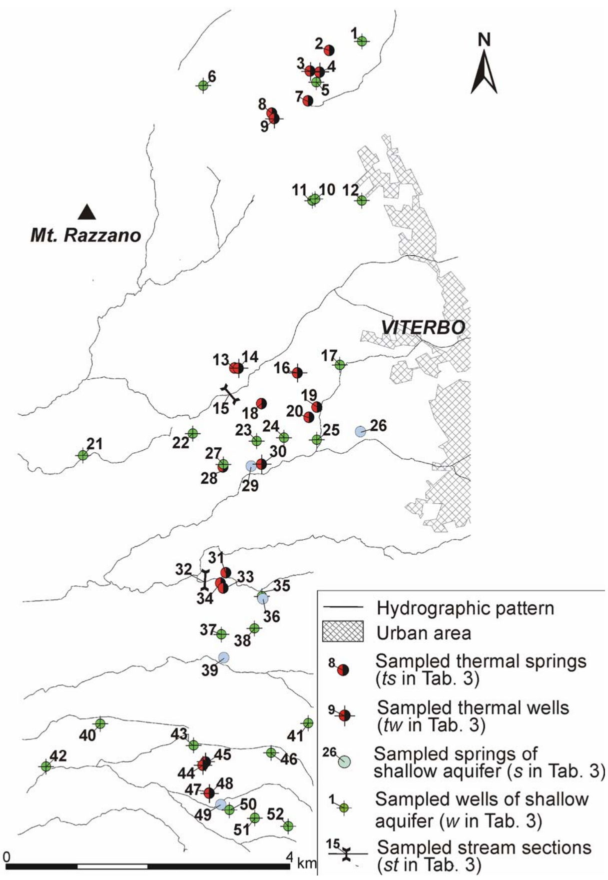

Figure 7. Location of sampled waters (IDs in Table 3).

Table 3. Main chemical constituents of sampled waters (June 2009).

ID	Type	T (˚C)	pH	EC (μS/cm)	Na^+ (mg/L)	K^+ (mg/L)	Ca^{2+} (mg/L)	Mg^{2+} (mg/L)	Cl^- (mg/L)	HCO_3^- (mg/L)	SO_4^{2-} (mg/L)	SiO_2 (mg/L)	Sr (mg/L)	F^- (mg/L)
1	*w*	24.0	7.31	1450	29	19	205	78	21.8	463	465	41.0	2.6	1.9
2 (Ba)	*ts*	50.0	6.70	3011	36	29	515	145	13.0	976	1100	43.3	11.4	4.0
3 (Ba)	*tw*	62.4	6.85	3290	49	30	504	150	16.2	1055	1155	47.5	11.6	3.9
4 (Ba)	*tw*	59.6	6.57	3300	36	29	508	145	17.8	1094	1140	47.3	11.4	4.2
5	*w*	17.0	7.40	1630	27	20	230	60	27.2	610	545	39.6	4.7	1.9
6	*w*	18.6	7.72	738	44	35	81	24	78.3	249	58	37.5	0.47	0.5
7 (Ba)	*ts*	33.6	6.20	3360	44	30	542	150	18.2	945	1300	40.3	12.2	3.2
8 (Ba)	*ts*	62.3	6.30	3170	35	28	487	150	14.4	985	1106	18.2	11.7	3.6
9 (Ba)	*tw*	61.7	6.32	2780	33	26	527	165	15.4	-	1270	40.3	11.3	4.7
10	*w*	29.4	6.10	2920	38.	28	468	115	23.8	1073	1023	29.6	9.7	1.5
11	*w*	25.2	6.20	2890	41	28	471	115	21.0	1061	956	40.0	9.9	1.3
12	*w*	17.0	7.80	535	41	16	43	12	19.0	189	53	39.3	2.2	3.6
13 (Bu)	*ts*	58.9	6.41	3230	34	29	500	141	15.2	1005	1115	45.0	12.1	4.2
14 (Bu)	*tw*	60.6	6.44	3200	34.	30	502	140	15.6	1018	1100	49.1	11.7	4.3
15	*st*	19.9	8.07	1255	44	21	168	40	49.4	457	282	39.4	2.7	1.9
16 (Bu)	*tw*	54.5	6.43	2900	34	31	456	115	17.6	1030	976	47.1	10.4	4.0
17	*w*	21.6	7.80	747	23	14	126	11	20.2	305	129	38.9	2.9	3.8
18 (Bu)	*ts*	57.8	6.40	3000	34	33	510	120	15.1	1067	986	48.2	11.1	3.3
19 (Bu)	*tw*	40.0	6.37	2770	34	27	496	109	17.0	976	946	45.2	9.5	2.6
20 (Bu)	*ts*	54.8	6.27	2990	35	30	500	115	12.3	1006	1091	53.6	11.1	4.0
21	*w*	21.3	7.71	756	46	26	73	14	21.6	177	141	40.2	0.60	4.0
22	*w*	21.6	6.93	1950	18	10	318	59	15.6	601	548	31.1	4.2	3.1
23	*w*	30.5	6.63	2880	30	24	507	112	17.0	1036	971	38.4	10.7	5.2
24	*w*	24.7	7.47	1697	27	34	225	110	14.0	378	650	39.4	6.9	2.4
25	*w*	20.0	7.40	1580	32	25	205	75	23.2	451	513	40.3	5.2	2.2
26	*s*	19.6	6.80	725	35	34	71	18	12.7	378	68	41.3	0.27	1.1
27	*w*	29.6	6.64	2480	38	16	465	55	48.0	754	912	43.3	5.6	3.6
28 (Ur)	*tw*	41.5	6.29	3490	67	28	588	140	20.4	1125	1299	41.3	12.2	4.4
29	*s*	31.4	6.63	2040	50	20	336	83	27.8	724	704	22.3	5.6	1.8
30 (Ur)	*tw*	52.5	6.37	3030	46	26	504	125	16.4	1021	1111	18.2	11.7	2.6
31 (Sc)	*ts*	53.6	6.40	3570	34	24	635	165	19.0	1066	1400	40.9	13.9	5.2
32	*st*	27.0	7.32	1930	34	22	302	72	21.4	549	769	38.9	5.5	3.2
33 (Sc)	*ts*	52.5	6.20	3520	31	26	618	150	15.6	1069	1401	51.3	13.3	3.6
34 (Sc)	*ts*	43.1	6.75	3560	30	26	584	150	15.0	1024	1346	44.2	13.7	3.1
35	*w*	21.1	7.45	393	23	21	43	10	28.2	140	42	36.6	0.34	1.8
36	*s*	16.0	7.77	490	28	10	36	11	29.1	116	46	39.5	0.54	0.5
37	*w*	25.0	8.37	350	17	18	27	8	15.6	132	18	34.5	0.17	0.8
38	*w*	21.3	7.80	532	25	20	46	11	42.7	52	57	37.6	0.38	1.1
39	*s*	17.0	7.86	327	25	22	15	8	23.1	101	19	31.3	0.17	0.8
40	*w*	20.8	6.64	1330	40	16	205	41	35.7	483	342	40.6	2.8	4.2
41	*w*	21.0	7.66	356	24	19	27	6	25.7	97	26	33.6	0.15	2.4
42	*w*	20.5	6.55	2360	27	24	376	90	21.0	729	952	42.3	8.0	4.0
43	*w*	20.2	7.88	880	9.3	4.6	157	10	12.0	354	69	42.0	1.3	1.7
44 (Pa)	*tw*	59.5	6.42	3540	43	26	637	155	23.2	1055	1405	39.8	13.2	3.4
45 (Pa)	*tw*	58.5	-	3230	32	26	632	170	19.6	-	1300	44.0	13.2	3.2
46	*w*	25.0	6.78	930	25	18	158	19	21.6	418	140	37.5	2.0	3.0
47	*s*	24.5	6.61	713	26	18	91	14	22.0	201	134	36.6	0.81	2.6
48 (Pa)	*tw*	58.2	6.39	3510	47	26	617	137	16.0	1069	1311	46.5	13.1	4.5
49	*s*	19.2	7.35	328	22	22	28	6	20.6	104	26	32.4	0.14	2.2
50	*w*	23.0	7.37	332	26	22	30	6	23.0	94	31	30.6	0.13	2.3
51	*w*	21.2	7.70	368	27	21	23	5	24.2	91	51	31.0	0.11	3.2
52	*w*	20.2	7.60	367	28	20	17	6	25.4	90	33	37.0	0.13	2.9

Ba: Bagnaccio Group; Bu: Bullicame Group; Ur: Urcionio Group; Sc: San Cristoforo Group; Pa: Paliano Group; *ts*: thermal spring; *tw*: thermal well; *s*: spring of the shallow aquifer; *w*: well of the shallow aquifer; *st*: stream section.

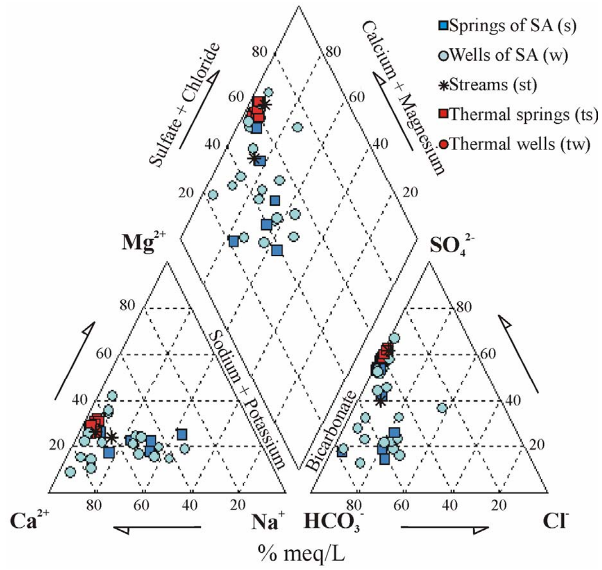

Figure 8. Piper diagram of sampled waters.

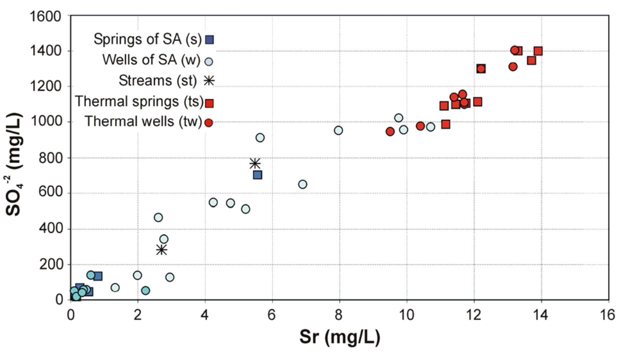

Figure 9. Plot of strontium versus sulfate contents of sampled waters.

$$\frac{Qt}{Qi} = \frac{Ci - Cc}{Ct - Cc}$$

The ratio Qt/Qi permits us to determine the fraction of thermal water in the groundwater of the SA. As reported in **Figure 10(a)**, Qt/Qi is between 0.1 and 0.5 in the central and northern zones of the Viterbo hydrothermal area and between 0.1 and 0.6 in the western zone beyond the boundary of the hydrothermal area. The same distribution of the Qt/Qi ratio is found when strontium is used as an indicator of the mixing between the thermal waters and cold waters of the SA (**Figure 10(b)**).

4.5. Stable Isotopes and Tritium

The stable isotopes of water ($\delta^{18}O$ and δ^2H), which were determined for thermal waters (2, 3, 4, 8, 9, 14, 16, 18, 19, 20, 30, 34, 44, 45, 48 in **Figure 7**), selected wells (6, 21, 23, 41 in **Figure 7**) and springs of the SA (26, 29, 39 in **Figure 7**) and two stream waters (15, 32 in **Figure 7**), are plotted in **Figure 11**. In the same graph, the global [65] and central-Italy meteoric water lines [66] and the isotopic contents of Vico Lake [37] are reported. All of the waters exhibit $\delta^{18}O$ and δ^2H values in a limited range (–5.6‰ to –7.2‰ and –34‰ to –44‰, respectively) and fall on the meteoric water lines, as determined by previous studies [37]. The waters with lower $\delta^{18}O$ values are from the TA and the basal water table of the SA. If the available vertical isotopic gradients for the western side of the Apennine Chain [66] are considered, then the elevation of the recharge area of the sampled waters ranges between 330 and 1270 m·asl. When only the waters that are more enriched in $\delta^{18}O$, *i.e.*, mainly those of the perched aquifers of the SA, are considered, the elevation is less than 470 m·asl.

The results for the stable isotopes of dissolved sulfate ($\delta^{34}S_{SO4}$ and $\delta^{18}O_{SO4}$) are plotted in **Figure 12**, which was modified from Clark and Fritz (1997) [67]. For the thermal waters, the $\delta^{34}S_{SO4}$ values vary from 11.4‰ to 16.8‰, and the $\delta^{18}O_{SO4}$ values vary from 11.3‰ and 14.2‰, with generally lower values for the SA and stream waters. According to the diagram of Clark and Fritz (1997) [67], the thermal waters plot within the Devonian to lower Triassic rectangle, in contrast to the SA and stream waters, which seem to be related to the atmospheric content or mixing with the two previous components. The Mesozoic-Cenozoic carbonate rocks, which constitute the deep substratum of the area under investigation, include Triassic anhydrites.

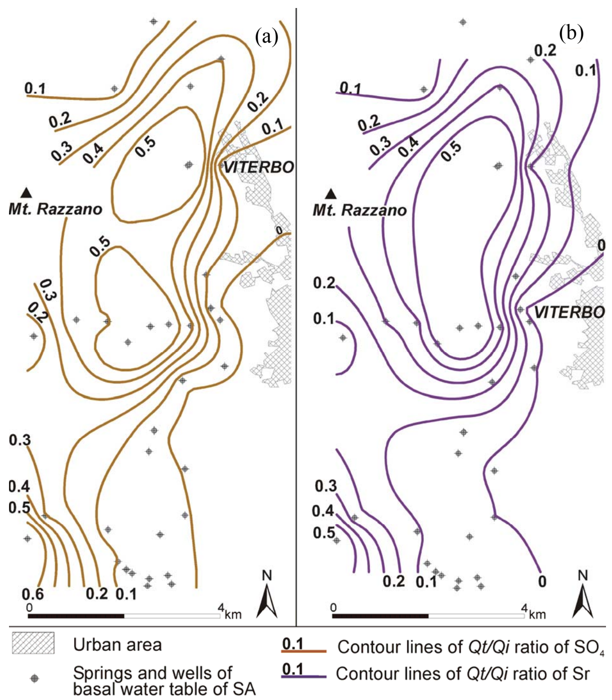

Figure 10. Map of the ratio *Qt/Qi* which represents the fraction of thermal water (*Qt*) in the groundwater of the SA (*Qi*), using (a) sulfate concentration and (b) strontium concentration.

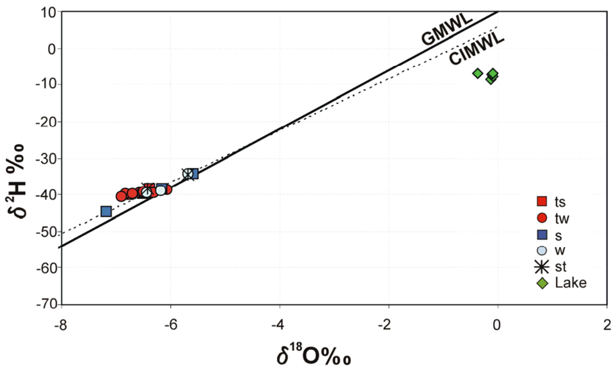

Figure 11. δ^{18}**O versus** δ^{2}**H in thermal waters (*ts* and *tw*), some wells (*w*) and springs (*s*) of SA and stream waters (*st*), compared with isotopic contents of waters of Vico Lake [37]. The global meteoric (GMWL) and central Italy meteoric water lines (CIMWL) are also shown.**

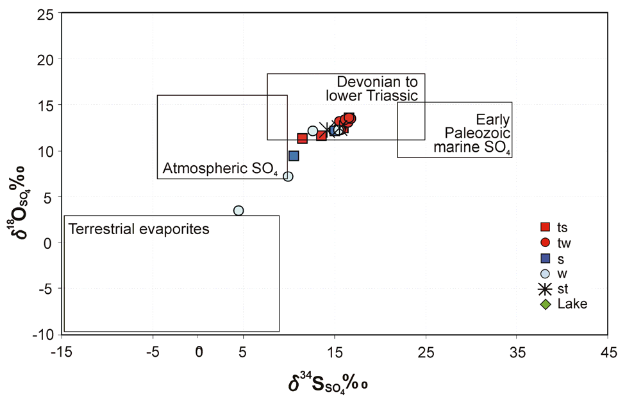

Figure 12. $\delta^{34}S_{SO4}$ **versus** $\delta^{18}O_{SO4}$ **in dissolved sulfate of thermal waters (*ts* and *tw*), some wells (*w*) and springs (*s*) of SA and stream waters (*st*) (fields from Clark and Fritz, 1997 [67]).**

As can be seen from the plot of **Figure 12**, some SA samples fall in the Devonian to lower Triassic rectangle, which again confirms the mixing with thermal waters.

Of the samples, 15 were analyzed for tritium, of which 12 were from thermal waters (2, 4, 8, 9, 14, 16, 18, 20, 30, 34, 45, 48 in **Figure 7**) and 3 were from cold waters (6, 21, 41 in **Figure 7**). The tritium concentrations varied from 2 to 11 TU, which suggests a recent component recharge of waters, *i.e.*, post-1952 [67]. The thermal waters had lower tritium concentrations (2 to 5 TU), whereas samples from wells exclusively intercepting the SA had higher concentrations (8 to 11 TU). If the radioactive half-life for tritium is considered and the same isotopic content of rainwater recharging is assumed for both thermal and cold waters, then there is a 14-year-difference in the residence time between the two types of waters.

4.6. Soil-Water Budget

The soil-water budget was estimated with reference to a surface area of approximately 38 km^2, including the strip where thermal waters flow out.

The mean annual values of precipitation and temperature for 1989 to 2010 were calculated by processing the meteorological data recorded in Viterbo. The homogeneity of the datasets was evaluated, and missing data were reconstructed on a monthly basis (2% of the precipitation data and 0.25% of the temperature data were missing). The mean annual values for precipitation and temperature are 772 mm and 15.7˚C, respectively.

Based on the mean monthly rainfall and temperature data, a potential evapotranspiration of 841 mm/y was calculated using the Thornthwaite empirical formula [68]. The actual evapotranspiration was also determined by the Thornthwaite-Mather method [69] by considering the soil texture, field capacity, permanent wilting point and land cover for the different zones in the area. The resulting total available water-holding capacity varies between 80 and 160 mm; therefore, the actual evapotranspiration varies between 525 and 605 mm/y.

The mean annual actual evapotranspiration is 575 mm for the strip where thermal waters flow out (surface area of 19.66 km^2), and the difference between the mean annual precipitation and actual evapotranspiration is 197 mm. For the northern and central zones of **Figure 10** with *Qt/Qi* between 0.1 and 0.5 (surface area of 18.79 km^2), the mean annual actual evapotranspiration is 581 mm, and the difference between the mean annual precipitation and actual evapotranspiration is 191 mm.

5. Discussion

A refinement of the conceptual model and a groundwater resource estimation of the Viterbo thermal area can be derived from the combination of hydrogeological and hydrochemical data.

The hydrogeological interpretation of the stratigraphy enables the characterization of the upper 100 - 200 m of the two main aquifers. The shallow aquifer (SA) consists of Pleistocene volcanites and covers the entire study area; the deeper aquifer (TA) is characterized by thermal waters. Within the study area, the two aquifers are generally separated by a low-permeability layer of volcanites or flysch units. At greater depths, a thick low-permeability layer consisting of flysch units is locally fractured and faulted and overlaps the deep carbonate rocks that are also faulted and dislocated (**Figure 13**).

The unconfined or leaky SA has a thickness of a few meters to tens of meters. The SA exhibits a piezometric surface that is consistent with that of the wide Cimino-Vico aquifer system. In the study area, the SA is recharged by direct infiltration and groundwater inflow from the Cimino-Vico system, discharges locally in streams and in springs, and westward groundwater outflow occurs. The

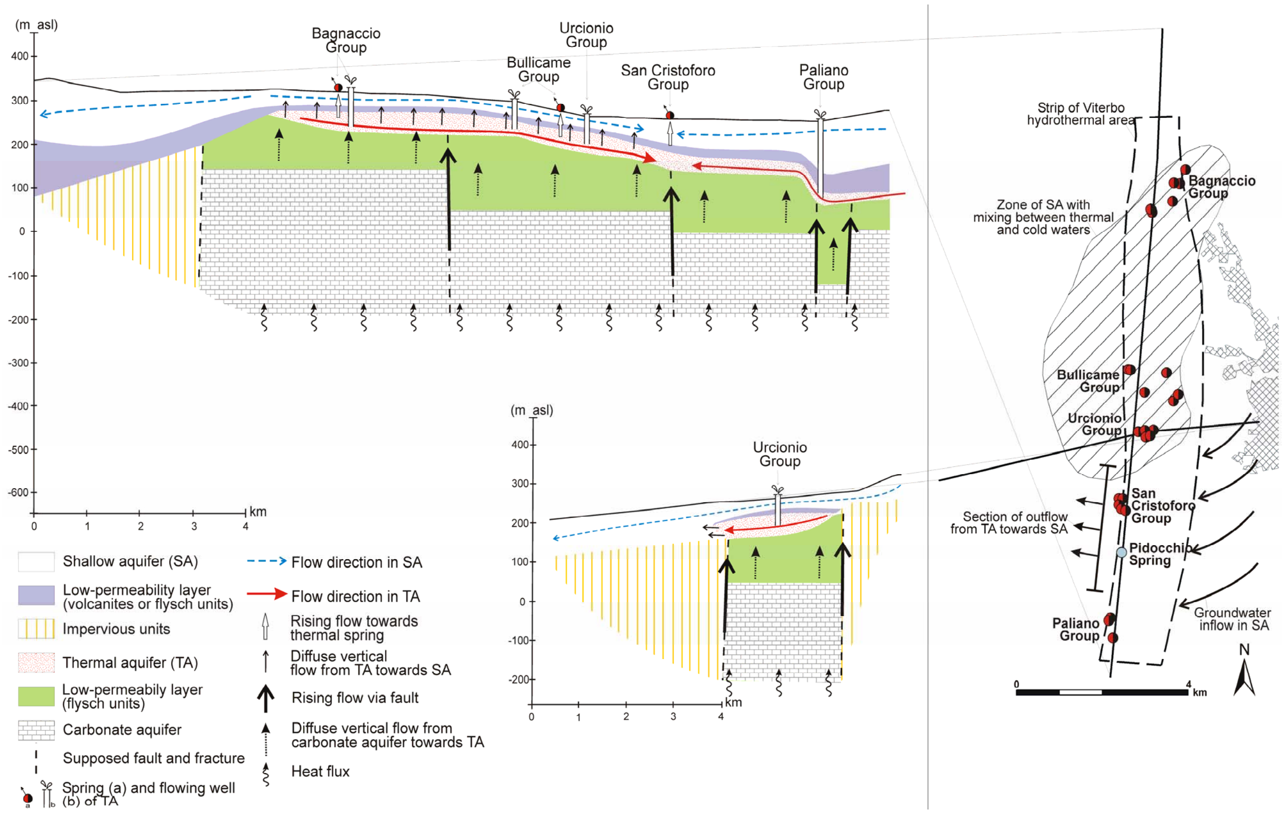

Figure 13. Hydrogeological conceptual model of the hydrothermal area of Viterbo showing the main groundwater paths in and among the overlapping aquifers. Zones considered for the evaluations of the yield of the groundwater system are shown on the right.

hydraulic parameters of the SA consist of transmissivity values between 10^{-5} m^2/s and 10^{-2} m^2/s and storativity values between 10^{-3} and 10^{-2}.

Waters circulating in the SA are generally characterized by low temperature (less than 23˚C) and salinity (EC less than 700 μS/cm) and are of bicarbonate-alkaline-earth or bicarbonate-alkaline types, which suggests a short duration of the rock-water interaction. Sampled waters from the SA included a hydrochemical facies that arose from mixing between typical cold waters and thermal waters. These waters have been found in the northern and central zones of the study area, where the SA overlies the TA, and in the western boundary of the hydrothermal area, where the TA has not been identified. In these zones, the flow from the TA influences 10% to 60% of the flow in the SA, based on sulfate and strontium concentrations.

The TA is located at a depth of up to 200 m and is characterized by thermal waters (T of 40˚C to 62˚C) with higher salinities (EC from 2800 to 3600 μS/cm). The thickness of the volcanites and flysch units constituting the TA varies between 50 and 80 m, even if other layers with thermal waters have been found in the same deep flysch units [53,54].

The TA has been identified within a rectangular area that is approximately 12 km long and 2 km wide (**Figure 13**), and it includes the following characteristics: 1) an uplift of sedimentary units underlying the volcanites; 2) a limited thickness of the same volcanic cover as the surroundings; 3) a fractured and faulted zone of the sedimentary basement; 4) a zone with one of the higher geothermal gradients in the Latium region (up to 100˚C /km) and, therefore, a high heat flow (from 100 to 400 mW/m^2) [1,26]; and 5) an outcropping of thermogene travertine and CO_2 emissions [33]. Within this N-S elongated zone, the TA is continuous (**Figure 13**). The southern boundary of the TA is not certain because the thermal waters have been intercepted by the Vico 2 Well in the volcanites (at a depth of 275 to 290 m) [57] and, recently, in the flysch units 10 km south of the area under investigation.

The confined TA is characterized by two main directions of flow that converge westwards, and its hydraulic parameters consist of transmissivity values of 10^{-2} m^2/s to 10^{-4} m^2/s and a storativity of approximately 10^{-4}. The hydraulic tests highlight the continuity of the TA and are in agreement with the results of production tests conducted in the 1950s [53,54].

The TA discharges into thermal springs and flowing wells. A diffuse vertical flow from the TA toward the SA through the aquitard also occurs, particularly in the northern and central zones of the strip where the two aquifers overlap, according to the vertical gradient between the two aquifers and the mixing highlighted by the chemical and isotopic data. Moreover, an outflow from the TA towards the SA occurs at its western boundary (**Figure 13**): 1) hydrostratigraphy highlights the lateral connection between the TA and the SA; 2) waters sampled from shallow wells show mixing with thermal waters; 3) the hydraulic heads of the TA and the SA are not as different. The northern and eastern boundaries of the TA do not present the full set of features.

Waters circulating in the TA are characterized by calcium-sulfate hydrochemical facies, a high dissolved gas content (CO_2 and H_2S), high temperature and salinity. These features, together with those obtained from the analyses of the minor and trace constituents (such as Sr and F^-), suggest deeper circuits and longer rock-water interactions compared with those occurring in the SA. The stability of the water quality based on the pumping tests and the chemical homogeneity of the thermal waters confirms the continuity of the TA. Isotopic analyses strengthen this hydrogeological conceptual model. The stable isotopes of water highlight the meteoric origin of the thermal waters and that their recharge area is similar to that of the SA. The waters of the two aquifers differ in residence time; the TA waters have an isotopic age of less than 50 - 60 years, which is approximately ten years older than the cold waters. Other chemical and isotopic indicators, such as the high sulfate and strontium content and $\delta^{34}S_{SO4}$ and $\delta^{18}O_{SO4}$ values, can be explained through interactions with the fluid circulating in the deep carbonate basement.

The deep carbonates were recognized as the main reservoir of hot fluids feeding geothermal wells in the Vulsini volcanic area e.g., [60,63], which is tens of kilometers from the study area. Documented evidence from four deep wells in and surrounding the area under examination confirms groundwater circulation in the carbonate aquifer [38,53,54,57]. Therefore, the deep carbonate aquifer can be considered to be a reservoir that recharges the TA, with a flow that mainly rises via faults and fractures in the sedimentary substratum of the volcanites because of the high heat flow that characterizes the region.

Considering the limited range of $\delta^{18}O$ and δ^2H in all waters sampled and the slight difference in tritium content between the thermal waters and those of the SA, the recharge area of the TA appears to be the same as that of the SA, *i.e.*, the Lake Vico area of the Cimini Mountains. According to Piscopo *et al*. (2006) [37], this circuit seems to be consistent with the difference between the hydraulic head of the recharge area (approximately 500 m·asl) and that determined for the thermal waters (from 225 and 320 m·asl).

Based on previous conceptual models, the yield of the groundwater system was estimated with reference to the strip (**Figure 13**) in which the thermal waters flow out (surface area of 19.66 km^2).

The total thermal water discharge (Q_{tw}) can be written as

$$Q_{tw} = Q_{sw} + Q_{vt} + Q_{lo} \quad (2),$$

where

Q_{sw} is the discharge into thermal springs and flowing wells;

Q_{vt} is the vertical flow from the TA towards the SA, which occurs in the northern and central zones of the strip; and

Q_{lo} is the flow from the TA towards the SA, which occurs mainly in the western boundary of the strip.

Q_{sw} is approximately 84 L/s, considering the average discharge measured in 1983-84 and 2008-10 (**Table 1**).

Q_{vt} can be evaluated by considering the direct infiltration in the northern and central zones of the SA (I_{nc}), where mixing between thermal and cold waters has been found (**Figure 13**), and the ratio of the flows of the two end members derived from Equation (1), rewritten as Qt/Qc:

$$Q_{vt} = I_{nc} \cdot \frac{Qt}{Qc}$$

I_{nc} was estimated to be approximately 91 L/s, taking into account the following: 1) the surface area where mixing has been found (18.79 km^2); 2) the mean annual difference between the precipitation and actual evapotranspiration calculated for the northern and central zones (191 mm); and 3) an I_{nc} equal to 0.8 of the difference between the precipitation and the actual evapotranspiration that is attributed to the flat topography of the area and the absence of streamflow for most of the year. The average Qt/Qc for the area under examination is 0.75, which gives a value of 68 L/s for Q_{vt}.

Q_{lo} can be evaluated by considering Qt/Qi for the western zone of the SA beyond the boundary of the strip and the horizontal flow in the SA, which corresponds to Qi, by applying Darcy's Law for the section of outflow from the TA toward the SA (**Figure 13**). Q_{lo} is approximately 53 L/s because the flow in the SA is approximately 220 L/s (if the mean transmissivity of this zone is considered, *i.e.*, the mean obtained from the PT6, SD5 and SD6 tests in **Table 2**), and the average Qt/Qi is 0.24.

The total discharge of the thermal waters, Q_{tw} is equal to 205 L/s.

The potential yield of the TA was independently estimated, taking into account the potentiometric surface and transmissivity values determined for the TA. Two sections of flow were considered according to the main flow directions. The first section is in the northern zone, and the second is in the southern zone of the strip; both sections were chosen to be distant from thermal springs and flowing wells. By assigning the lower values obtained from the pumping tests of the northern and southern sections and the proper values of the hydraulic gradient, a total flow rate of approximately 250 L/s results from the application of Darcy's Law.

Although these evaluations may be subject to uncertainty because of the methods employed and the uncertainty in the data, it is clear that the yield of the TA is higher than what is discharged into the springs and wells. The TA can be considered to have a minimum yield of approximately 170 L/s in the examined strip, even with a 30% error in Equation (2) (*i.e.*, Q_{vt} and Q_{lo}).

To complete the evaluation of the yield of the groundwater system, the mean potential direct recharge was estimated for the SA in the strip under examination. The result was approximately 98 L/s, which considers the mean annual difference between the precipitation and the actual evapotranspiration of the entire strip. The yield of the SA in the strip is higher than the direct recharge because of the groundwater inflow from the Cimino-Vico system in the eastern boundary of the strip. In the strip, the effective irrigation consumption from the SA can be evaluated by taking into account the difference between the potential (841 mm) and actual evapotranspiration (577 mm) of the irrigated zones included in the strip (12.46 km^2) and considering that the over-irrigation returns to the shallow aquifer. The estimated effective irrigation consumption is 104 L/s, which is comparable to the direct recharge.

6. Conclusions

The hydrogeological conceptual model seems to be more complex than the models presented previously in the literature. The shallowest 100 - 200 m of the two main aquifers, which are mainly tapped for drinking water, irrigation and spas, have been characterized. At a greater depth, another aquifer was recognized as the reservoir of the hot waters feeding the shallower waters. The hydraulic and chemical characteristics of the two shallower aquifers that were examined in detail in this study are very different. The first aquifer (SA) is related to the regional groundwater flow of the Cimino-Vico system, is hydraulically heterogeneous and is generally characterized by cold, fresh waters. The second aquifer (TA) is continuous within a strip in which the local hydrostratigraphic, structural and geothermal conditions allow a relatively active and constantly replenished flow of thermal waters with higher salinity. These two aquifers interact vertically and laterally, to give rise to mixed waters circulating in the first aquifer.

The yield of the groundwater system was estimated by an integrated hydrogeological and hydrochemical approach. In the examined strip, the yield of the TA is at least 170 L/s, and it discharges into thermal springs and wells and feeds the SA vertically and laterally. The SA is recharged by direct infiltration and inflow from regional groundwater as well as inflow from the second aquifer.

Based on the conceptual hydrogeological model and the previous estimate of the yield of the groundwater system, some preliminary considerations regarding groundwater management can be made.

Even if, at the scale of the whole groundwater flow system, the potential exists for future development of the TA, then an increase in withdrawals through wells from the TA could result in a decrease in the discharge from the thermal springs, which has occurred in the past for some thermal springs and was verified during the pumping tests. Therefore, the future use of thermal waters must account for the potential yield of the TA and provide sufficient residual discharge at thermal springs for recreational use.

The effects of withdrawals from the SA on the entire groundwater system may also be important if it is considered that the flow rate necessary for irrigation in the strip is comparable to the direct recharge in the area. At the local scale, pumping from the SA could increase the vertical gradient between the two overlapping aquifers to cause an increase in flow from the TA toward the SA. This could cause an increase in the temperature and salinity of the SA that is tapped for irrigation and drinking water as well as a decrease in the flow rate of the thermal waters tapped to supply spas and for recreational use.

These examples highlight that, in the volcanic hydrogeological environment, one of the most stringent constraint in determining the correct usage of a resource is the co-existence of interacting groundwater flows of different qualities. However, in this fragile and complex hydrogeological system with a multi-purpose water demand, future decisions regarding groundwater management must also be based on economic, legal and environmental criteria to define the priorities for the use of different groundwater resources.

7. Acknowledgements

The authors are thankful to the Regione Lazio—Direzione Regionale Attività Produttive e Rifiuti, in the persons of Dr Mario Marotta, Eng Luigi Minicillo and Dr Patrizia Refrigeri, and Ministero dell'Istruzione, dell'Università e della Ricerca (Project PRIN-2008 - 2008YYZKEE_02) for financial support.

REFERENCES

[1] R. Cataldi, M. Mongelli, P. Squarci, L. Taffi, G. Zito and C. Calore, "Geothermal Ranking of Italian Territory," *Geothermics*, Vol. 24, No. 1, 1995, pp. 115-129. doi:10.1016/0375-6505(94)00026-9

[2] G. Bertrand, H. Celle-Jeanton, F. Huneau, S. Loock and

C. Renac, "Identification of Different Groundwater Flowpaths within Volcanic Aquifers Using Natural Tracers for the Evaluation of the Influence of Lava Flows Morphology (Arghat Basin, Chaîne des Puys, France)," *Journal of Hydrology*, Vol. 391, No. 3-4, 2010, pp. 223-234. doi:10.1016/j.jhydrol.2010.07.021

[3] J. V. Cruz and M. O. Silva, "Hydrogeologic Framework of the Pico Island (Azores, Portugal)," *Hydrogeology Journal*, Vol. 9, No. 2, 2001, pp. 177-189. doi:10.1007/s100400000106

[4] E. Custodio, "Groundwater Characteristics and Problems in Volcanic Rock Terrains," In: IAEA, *Isotope Techniques on the Study of the Hydrology of Fractured and Fissured Rocks*, STI/PUB 790, Vienna, 1989, pp. 87-137.

[5] E. Custodio, "Groundwater in Volcanic Rocks," In: Krasny, J. and J. M. Sharp, Eds., *Groundwater in Fractured Rocks*, Taylor and Francis Group, London, 2007

[6] V. Piscopo, V. Allocca and F. Formica, "Sustainable Management of Groundwater in Neapolitan Volcanic Areas, Italy," In: O. Sililo, *et al*., Eds., *Groundwater*: *Past Achievements and Future Challenge*, Balkema, Rotterdam, 2000.

[7] V. Piscopo, A. Baiocchi, S. Bicorgna and F. Lotti, "Hydrogeological Support for Estimation of the Sustainable Well Yield in Volcanic Rocks: Some Examples from Central and Southern Italy," *Proceedings of* 36*th IAH Congress on Integrating Groundwater Science and Human Well-Ceing*, Toyama, 26 October-1 November 2008, pp. 1652-1666.

[8] P. Ambrosetti, M. G. Carboni, M. A. Conti, A. Costantini, U. Esu Nicosia, G. Parisi and F. Sandrelli, "Evoluzione Paleogeografica e Tettonica dei BAcini Tosco-Umbro Laziali nel Pliocene e Nel Pleistocene Inferiore," *Memorie della Società Geologica Italiana*, Vol. 19, 1978, pp. 573-580.

[9] P. Baldi, F. A. Decandia, A. Lazzarotto and A. Calamai, "Studio Geologico del Substrato della Copertura Vulcanica Laziale Nella Zona dei Laghi di Bolsena, Vico e Bracciano," *Memorie Società Geologica Italiana*, Vol. 13, No. 4, 1974, pp. 575-606.

[10] F. Barberi, G. Buonasorte, R. Cioni, A. Fiordelisi, L. Foresi, S. Iaccarino, M. A. Laurenzi, A. Sbrana, L. Vernia and I. M. Villa, "Plio-Pleistocene Geological Evolution of the Geothermal Area of Tuscany and Latium," *Memorie Descrittive della Carta Geologica d'Italia*, Vol. 49, 1994, pp. 77-134.

[11] G. Marinelli, F. Barberi and R. Cioni, "Sollevamenti Neogenici e intrusioni acide della Toscana e del Lazio settentrionale," *Memorie della Società Geologica Italiana*, Vol. 49, 1993, pp. 279-288.

[12] L. Beccaluva, P. Di Girolamo and G. Serri, "Petrogenesis and Tectonic Setting of the Roman Volcanic Province, Italy," *Lithos*, Vol. 26, No. 3-4, 1991, pp. 191-221. doi:10.1016/0024-4937(91)90029-K

[13] S. Conticelli and A. Peccerillo, "Petrology and Geochemistry of Potassic and Ultrapotassic Volcanism in Central Italy: Petrogenesis and Inferences on the Evolution of the Mantle Sources," *Lithos*, Vol. 28, No. 3-6, 1992, pp. 221-240. doi:10.1016/0024-4937(92)90008-M

[14] G. Marinelli, "Magma Evolution in Italy," In: C. H. Squyres, Ed., *Geology of Italy*, The Earth Science Society of the Lybian Arab Republic, Tripoli, 1975, pp. 165-219.

[15] A. Peccerillo and P. Manetti, "The Potassium Alkaline Volcanism of Central-Southern Italy: A Review of the Data Relevant to Petrogenesis and Geodynamic Significance," *Transactions of the Geological Society of South Africa*, Vol. 88, No. 2, 1985, pp. 379-384.

[16] C. Cimarelli and D. de Rita, "Structural Evolution of the Pleistocene Cimini Trachytic Volcanic Complex (Central Italy)," *Bulletin of Volcanology*, Vol. 68, No. 6, 2006, pp. 538-548. doi:10.1007/s00445-005-0028-3

[17] D. Lardini and G. Nappi, "I Cicli Eruttivi del Complesso Vulcanico Cimino," *Rendiconti della Società Italiana di Mineralogia e Petrologia*, Vol. 42, 1987, pp. 141-153.

[18] F. Sollevanti, "Geologic, Volcanologic and Tectonic Setting of the Vico-Cimino Area, Italy," *Journal of Volcanology and Geothermal Research*, Vol. 17, No. 1-4, 1983, pp. 203-217. doi:10.1016/0377-0273(83)90068-9

[19] A. Bertagnini and A. Sbrana, "Il Vulcano di Vico: Stratigrafia del Complesso Vulcanico e Sequenze Eruttive Delle Formazioni Piroclastiche," *Memorie della Società Geolologica Italiana*, Vol. 35, No. 2, 1986, pp. 699-713.

[20] G. Nappi, L. Valentini and M. Mattioli, "Ignimbritic Deposits in Central Italy: Pyroclastic Products of the Quaternary Age and Etruscan Footpaths. Field Trip Guide Book—P09," Proceedings 32*nd International Geological Congress*, Florence, 20-28 August 2004, p. 32.

[21] G. Perini, S. Conticelli and L. Francalanci, "Inferences of the Volcanic History of the Vico Volcano, Roman Magmatic Province, Central Italy: Stratigraphic, Petrographic and Geochemical Data," *Mineralogica et Petrographica Acta*, Vol. 15, 1997, pp. 67-93.

[22] G. Buonasorte, M. G. Carboni and M. A. Conti, "Il Substrato Plio-Pleistocenico Delle Vulcaniti Sabatine: Considerazioni Stratigrafiche e Paleoambientali," *Bollettino della Società Geologica Italiana*, Vol. 110, No. 1, 1991, pp. 35-40.

[23] R. Funiciello, E. Locardi, G. Lombardi and M. Parotto, "The Main Volcanic Groups of Latium. Relations between Structural Evolution and Petrogenesis," *Geologica Romana*, Vol. 15, 1976, pp. 279-300.

[24] P. La Torre, R. Nannini and F. Sollevanti, "Geothermal Exploration in Central Italy: Geophysical Survey in Cimini Range Area," *European Association of Exploration Geophysicists*: 43*th Meeting*, Venezia, 26-29 May 1981.

[25] G. Buonasorte, A. Fiordelisi, E. Pandeli, U. Rossi and F. Sollevanti, "Stratigraphic Correlations and Structural Setting of the Pre-Neoautochtonous Sedimentary Sequences of Northern Latium," *Periodico di Mineralogia*, Vol. 56, 1987, pp. 111-122.

[26] A. Calamai, R. Cataldi, E. Locardi and A. Praturlon, "Distribuzione Delle Anomalie Geotermiche Nella Fascia Preappenninica Tosco-Laziale (Italia)," *Symposium International Sobre Energia Geotérmica en America Latina*, Ciudad de Guatemala, 16-23 October 1976, pp. 189-229.

[27] B. Della Vedova, G. Pellis, J. P. Foucher and J. P Rehault, "Geothermal Structure of Tyrrhenian Sea," *Marine Geology*, Vol. 55, No. 3-4, 1984, pp. 271-289.

doi:10.1016/0025-3227(84)90072-0

[28] F. Mongelli, G. Zito, N. Ciaranfi and P. Pieri, "Interpretation of Heat Flow Density of the Apennine Chain, Italy," *Tectonophysics*, Vol. 164, No. 2-4, 1989, pp. 267-280. doi:10.1016/0040-1951(89)90020-6

[29] G. Chiodini, F. Frondini and L. Marini, "Theoretical Geothermometers and P_{CO_2} Indicators for Aqueous Solutions Coming from Hydrothermal Systems of Medium-Low Temperature Hosted in Carbonate-Evaporite Rocks. Application to the Thermal Springs of the Etruscan Swell, Italy," *Applied Geochemistry*, Vol. 10, No. 3, 1995, pp. 337-346. doi:10.1016/0883-2927(95)00006-6

[30] G. Chiodini, F. Frondini and F. Ponziani, "Deep Structures and Carbon Dioxide Degassing in Central Italy," *Geothermics*, Vol. 24, No. 1, 1995, pp. 81-94. doi:10.1016/0375-6505(94)00023-6

[31] V. Duchi and A. Minissale, "Distribuzione Delle Manifestazioni Gassose Nel Settore Peritirrenico Tosco-Laziale e Loro Interazione con gli Acquiferi Superficiali," *Bollettino della Società Geologica Italiana*, Vol. 114, No. 2, 1995, pp. 337-351.

[32] A. Minissale and V. Duchi, "Geothermometry on Fluids Circulating in a Carbonate Reservoir in North-Central Italy," *Journal of Volcanology and Geothermal Research*, Vol. 35, No. 3, 1988, pp. 237-252. doi:10.1016/0377-0273(88)90020-0

[33] A. Minissale, D. M. Kerrick, G. Magro, M. T. Murell, M. Paladini, S. Rihs, N. C. Sturchio, F. Tassi and O. Vaselli, "Geochemistry of Quaternary Travertines in the Region North of Rome (Italy): Structural, Hydrologic and Paleoclimatic Implications," *Earth and Planetary Science Letters*, Vol. 203, No. 2, 2002, pp. 709-728. doi:10.1016/S0012-821X(02)00875-0

[34] A. Baiocchi, W. Dragoni, F. Lotti, G. Luzzi and V. Piscopo, "Outline of Theology of the Cimino and Vico Area and of the Interaction between Groundwater and Lake Vico (Lazio Region, Central Italy)," *Bollettino della Società Geologica Italiana*, Vol. 125, No. 2, 2006, pp. 187-202.

[35] C. Boni, P. Bono and G. Capelli, "Schema Idrogeologico Dell'Italia Centrale," *Memorie della Società Geologica Italiana*, Vol. 35, No. 2, 1986, pp. 991-1012.

[36] G. Capelli, R. Mazza and C. Gazzetti, "Strumenti e Strategie per la Tutela e l'uso Compatibile Della Risorsa Idrica del Lazio: Gli Acquiferi Vulcanici," Pitagora, Bologna, 2005.

[37] V. Piscopo, M. Barbieri, V. Monetti, G. Pagano, S. Pistoni, E. Ruggi and D. Stanzione, "Hydrogeology of Thermal Waters in Viterbo Area, Central Italy," *Hydrogeology Journal*, Vol. 14, No. 8, 2006, pp. 1508-1521. doi:10.1007/s10040-006-0090-8

[38] U. Chiocchini, F. Castaldi, M. Barbieri and V. Eulilli, "A Stratigraphic and Geophysical Approach to Studying the Deep-Circulating Groundwater and Thermal Springs, and Their Recharge Areas, in Cimini Mountains-Viterbo Area, Central Italy," *Hydrogeology Journal*, Vol. 18, No. 6, 2010, pp. 1319-1341. doi:10.1007/s10040-010-0601-5

[39] P. Baldi, G. C. Ferrara, L. Masselli and G. Pieretti, "Hydrogeochemistry of the Region between Monte Amiata and Rome," *Geothermics*, Vol. 2, No. 3-4, 1973, pp. 124-141. doi:10.1016/0375-6505(73)90020-5

[40] M. Angelone, C. Cremisini, V. Piscopo, M. Proposito and F. Spaziani, "Influence of Hydrostratigraphy and Structural Setting on the Arsenic Occurrence in Groundwater of the Cimino-Vico Volcanic Area (Central Italy)," *Hydrogeology Journal*, Vol. 17, No. 4, 2009, pp. 901-914. doi:10.1007/s10040-008-0401-3

[41] G. Capasso and S. Inguaggiato, "A Simple Method for the Determination of Dissolved Gases in Natural Waters. An Application to Thermal Waters from Volcano Island," *Applied Geochemistry*, Vol. 13, No. 5, 1998, pp. 631-642. doi:10.1016/S0883-2927(97)00109-1

[42] S. Epstein and T. Mayeda, "Variation of ^{18}O Content of Water from Natural Sources," *Geochimica et Cosmochimica Acta*, Vol. 4, No. 5, 1953, pp. 213-224. doi:10.1016/0016-7037(53)90051-9

[43] F. Yanagisawa and H. Sakai, "Preparation of SO_2 for Sulfur Isotope Ratio Measurements by the Thermal Decomposition of $BaSO_4$-V_2O_5-SiO_2 Mixtures," *Analytical Chemistry*, Vol. 55, No. 6, 1983, pp. 985-987. doi:10.1021/ac00257a046

[44] M. P. Neary, "Tritium Enrichment—To Enrich or Not to Enrich?" *Radioactivity and Radiochemistry*, Vol. 8, 1997, pp. 23-35.

[45] SIMN, "Annali Idrologici," Servizio Idrografico e Mareografico Nazionale, Ministero dei Lavori Pubblici, Roma, 1951-1999.

[46] Regione Lazio, "Annali Idrologici," Ufficio Idrografico e Mereografico Regione Lazio, Roma, 2000-2010.

[47] G. Allen, S. Pereira, D. Raes and M. Smith, "Crop Evapotranspiration—Guidelines for Computing Crop Water Requirements," Natural Resources Management and Environment Department, FAO, Rome, 1998.

[48] C. T. Haan, "Statistical Methods in Hydrology," The Iowa State University Press, Ames, 1977.

[49] S. Carnicelli, D. Sagri, U. Chiocchini and S. Madonna, "Geopedologia," In: U. Chiocchini, Ed., *La Geologia Della Città di Viterbo*, Cangemi Editore, Roma, 2004.

[50] P. Lorenzoni, M. Raglione, P. Quantin, D. Bidini and L. Lulli, "Studio Dell'Apparato Vulcanico di Vico (Lazio). IV. I Suoli Delle Colate Piroclastiche," *Annali Istituto Sperimentale di Studio e Difesa Suolo Firenze*, Vol. 16, 1985, pp. 199-226.

[51] L. Lulli, C. Blasi, G. Abate, D. Bidini, S. Fascetti, P. Lorenzoni and M. Marchetti, "Studio Pedologico Dell'Apparato Vulcanico di Vico (Lazio). VIII. L'effetto Della Vegetazione Sulla Genesi dei Suoli," *Annali Istituto Sperimentale di Studio e Difesa Suolo Firenze*, Vol. 17, 1986, pp. 159-172.

[52] Regione Lazio, "Carta di Uso del Suolo," Direzione Regionale Territorio e Urbanistica, Regione Lazio, Roma, 2003.

[53] B. Conforto, "Risultati Della Prima Fase di Ricerche di Forze Endogene nel Viterbese," *L'Ingegnere*, Vol. 27, 1954, pp. 345-350.

[54] B. Conforto, "Risultati Della Prima Fase di Ricerche di Forze Endogene nel Viterbese," *L'Ingegnere*, Vol. 27,

1954, pp. 521-530.

[55] P. P. Mattias and V. Ventriglia, "La Regione Vulcanica dei Monti Cimini e Sabatini," *Memorie della Società Geologica Italiana*, Vol. 9, No. 3, 1970, pp. 331-384.

[56] B. Toro, "Anomalie Residue di Gravità e Strutture Profonde Nelle Aree Vulcaniche del Lazio Settentrionale," *Geologica Romana*, Vol. 17, 1978, pp. 35-44.

[57] B. Camponeschi and F. Nolasco, "Le Risorse Naturali Della Regione Lazio. 2 Monti Cimini e Tuscia Romana," Regione Lazio, Roma, 1984.

[58] G. Buonasorte, R. Cataldi, A. Ceccarelli, A. Costantini, S. D'Offizi, A. Lazzarotto, A., Ridolfi, P. Baldi, A. Borelli, G. Bertini, R. Bertrami, A. Calamai, G. Cameli, R. Corsi, C. D'Acquino, A. Fiordelisi, A. Grezzo and F. Lovari, "Ricerca ed Esplorazione Nell'Area Geotermica di Torre Alfina (Lazio—Umbria)," *Bollettino della Società Geologica Italiana*, Vol. 107, No. 2, 1988, pp. 265-337.

[59] G. Buonasorte, E. Pandeli and A. Fiordelisi, "The Alfina 15 Well: Deep Geological Data from Northern Latium (Torre Alfina Geothermal Area)," *Bollettino della Società Geologica Italiana*, Vol. 110, No. 3-4, 1991, pp. 823-831.

[60] R. Cataldi and M. Rendina, "Recent Discovery of a New Geothermal Field: Alfina," *Geothermics*, Vol. 2, No. 3-4, 1973, pp. 106-116. doi:10.1016/0375-6505(73)90016-3

[61] G. Cavarretta, G. Giannelli, G. Scandiffio and F. Tecce, "Evolution of the Latera Geothermal System II: Metamorphic Hydrothermal Mineral Assemblages and Fluid Chemistry," *Journal of Volcanology and Geothermal Research*, Vol. 26, No. 3-4, 1985, pp. 337-364. doi:10.1016/0377-0273(85)90063-0

[62] V. Duchi, L. Matassoni, F. Tassi and B. Nisi, "Studio Geochimico dei Fluidi (Acque e Gas) Circolanti Nella Regione Vulcanica dei M.ti Vulsini (Italia Centrale)," *Bollettino della Società Geologica Italiana*, Vol. 122, No. 1, 2003, pp. 47-61.

[63] G. Giannelli and G. Scandiffio, "The Latera Geothermal System (Italy): Chemical Composition of the Geothermal Fluid and Hypotheses on Its Origin," *Geothermics*, Vol. 18, No. 3, 1989, pp. 447-463. doi:10.1016/0375-6505(89)90068-0

[64] G. F. Pinder and J. F. Jones, "Determination of the Groundwater Component of Peak Discharge from Chemistry of Total Runoff," *Water Resources Research*, Vol. 5, No. 2, 1969, pp. 438-445. doi:10.1029/WR005i002p00438

[65] H. Craig, "Isotopic Variations in Meteoric Water," *Science*, Vol. 133, No. 3465, 1961, pp. 1702-1703. doi:10.1126/science.133.3465.1702

[66] A. Longinelli and E. Selmo, "Isotopic Composition of Precipitation in Italy: A First Overall Map," *Journal of Hydrology*, Vol. 270, No. 1-2, 2003, pp. 75-88.

[67] I. D. Clark and P. Fritz, "Environmental Isotopes in Hydrogeology," Lewis Publishers, New York, 1997.

[68] C. W. Thornthwaite, "An Approach toward a Rational Classification of Climate," *Geographical Review*, Vol. 38, No. 1, 1948, pp. 55-94. doi:10.2307/210739

[69] C. W. Thornthwaite and J. R. Mather, "The Water Balance," *Publication in Climatology*, Vol. 8, No. 1, 1955.